

# Influence of Slag and Refractory Materials on Inclusions during the Ladle Refining of Low Carbon Aluminum Killed Steel

Fubin Gao <sup>1,2</sup>, Fuming Wang <sup>1,\*</sup>, Min Jiang <sup>1</sup>, Jianli Li <sup>2,3</sup>  and Xiang Zhang <sup>2,3</sup> 

<sup>1</sup> School of Metallurgical and Ecological Engineering, University of Science and Technology Beijing, 30 Xueyuan Road, Beijing 100083, China

<sup>2</sup> Handan Iron and Steel Company Hegang Group, 232 Fuxing Road, Handan 056015, China

<sup>3</sup> The State Key Laboratory of Refractories and Metallurgy, Wuhan University of Science and Technology, Wuhan 430081, China

\* Correspondence: wangfuming@metall.ustb.edu.cn

**Abstract:** The evolution of inclusions in low carbon Al killed steel during ladle refining of was studied based on industrial experiments, in which high basicity slag was used. The results showed that inclusions experienced the changes from  $\text{Al}_2\text{O}_3 \rightarrow \text{MgO-Al}_2\text{O}_3 \rightarrow \text{CaO-MgO-Al}_2\text{O}_3 \rightarrow \text{CaO-Al}_2\text{O}_3$ . Without calcium treatment,  $\text{MgO-Al}_2\text{O}_3$  inclusion in steel were largely transformed into  $\text{CaO-MgO-Al}_2\text{O}_3$  or  $\text{CaO-Al}_2\text{O}_3$ . With the aim to decrease  $\text{MgO-Al}_2\text{O}_3$  inclusions and to clarify the effects of refining slag and refractory materials on inclusions, laboratory experiments were performed with lower basicity refining slag (lower basicity slag theoretically helps reduce spinel-type inclusions) in  $\text{MgO}$  and  $\text{Al}_2\text{O}_3$  crucibles. The results indicated that, the dissolved Al in liquid steel would react with  $\text{MgO}$  and  $\text{CaO}$  in slag or in refractory at  $1600^\circ\text{C}$ . Hence,  $[\text{Mg}]$  and  $[\text{Ca}]$  would be supplied into bulk steel. Due to the large contact area between  $\text{MgO}$ -based refractory and steel, as well as the higher activity of  $\text{MgO}$  in the refractory, Mg can be more easily reduced, which accounts for the easy modification of  $\text{Al}_2\text{O}_3$  into  $\text{MgO-Al}_2\text{O}_3$ . By contrast, because of the limited supply of  $[\text{Ca}]$  to steel, modification of  $\text{MgO-Al}_2\text{O}_3$  into  $\text{CaO-MgO-Al}_2\text{O}_3$  or  $\text{CaO-Al}_2\text{O}_3$  was incomplete. With the use of  $\text{Al}_2\text{O}_3$ -based refractory and reeving slag basicity of about 2.45,  $\text{MgO-Al}_2\text{O}_3$  inclusions were obviously decreased.

**Keywords:** low carbon steel; Aluminium deoxidation; LF refining; inclusions; calcium treatment



**Citation:** Gao, F.; Wang, F.; Jiang, M.; Li, J.; Zhang, X. Influence of Slag and Refractory Materials on Inclusions during the Ladle Refining of Low Carbon Aluminum Killed Steel.

*Metals* **2023**, *13*, 866. <https://doi.org/10.3390/met13050866>

Academic Editors: Lauri Holappa and Mark E. Schlesinger

Received: 2 March 2023

Revised: 1 April 2023

Accepted: 24 April 2023

Published: 29 April 2023



**Copyright:** © 2023 by the authors. Licensee MDPI, Basel, Switzerland. This article is an open access article distributed under the terms and conditions of the Creative Commons Attribution (CC BY) license (<https://creativecommons.org/licenses/by/4.0/>).

## 1. Introduction

Low carbon aluminum killed steel (LCAK) with good toughness, ductility, stamping, surface and aging resistance is mainly used to manufacture automobiles, household appliances, etc. [1–4]. To ensure the properties, size, quantity and shape of inclusions in steel should be strictly controlled, lower contents of  $\text{O}_{\text{tot}}$  (total oxygen) and N are necessary [5–7].

During continuous casting, LCAK usually has poor castability due to the easy occurrence of clogging problems, which are often initiated by solid inclusions such as  $\text{Al}_2\text{O}_3$  and  $\text{MgO-Al}_2\text{O}_3$  in steel. To improve castability of liquid steel, calcium treatment is often adopted during ladle furnace (LF) refining by modifying such solids into semi-liquid or liquid states [8–16]. However, the yield ratio of Ca is usually unstable because of its high vaporization pressure at high temperatures [17–20]. Moreover, the application of calcium treatment means higher costs and longer production times. Furthermore, the addition of Ca into liquid steel often causes environmental problems such as smoke in production sites.

Hence, improving the castability of LCAK without the use of calcium treatment is very significant for its industrial production. However, the challenge is: how to modify the solid inclusions into liquid states without calcium treatment.

Holappa [17] et al. found that contents of  $\text{O}_{\text{tot}}$  and  $[\text{S}]$  in steel significantly influence modifications of inclusions in calcium treatment. When  $[\text{S}]$  content in steel is constant, the lower the content of  $\text{O}_{\text{tot}}$  in molten steel, the narrower the “window” of  $[\text{Ca}]$  content required for the formation of liquid inclusion. When the content of  $\text{O}_{\text{tot}}$  is constant, with the

rise of [S] content in steel, the narrower the “window” of [Ca] required for the formation of liquid inclusions. Pretorius [18] et al. found that calcium treatment could improve the castability of steel, but it would be hard to fully liquify MgO-Al<sub>2</sub>O<sub>3</sub> at a low melting point. During calcium treatment, calcium would preferentially react with magnesium oxide in the inclusions, but the free magnesium produced after the reaction would produce new MgO-Al<sub>2</sub>O<sub>3</sub> inclusions with aluminum oxide in molten steel. During casting, the re-oxidation of steel causes large formations of solid calcium-aluminates [19,20]. Park proposed that refining the slag of CaO-Al<sub>2</sub>O<sub>3</sub>-MgO system with a mass ratio of CaO/SiO<sub>2</sub> over 6.0 helps to modify inclusions in stainless steel from solid to liquid states [21].

Most studies on targeting liquid inclusions in Al steel mainly focused on calcium treatment. Additionally, CaO-Al<sub>2</sub>O<sub>3</sub>-MgO system refining slag is seldom used in LCAK. Hence, enhancing castability of LCAK without the application of calcium treatment is needed for industrial production. Considering that, the present study was carried out.

## 2. Experiments and Sample Analysis

### 2.1. Industrial Test

LCAK steel (SPHC) was produced by “BOF → LF refining → CC (the section sizes of the slab were about 1400 mm × 240 mm)”. Operations in the refining process included: (1) The carried slag from the tapping was removed from the ladle. MgO-C refractory was used at the slag line of the ladle, while MgO-Al<sub>2</sub>O<sub>3</sub> refractory bricks (MgO content was about 10%) were chosen as the lining for other parts of the ladle. (2) Aluminum, ferromanganese alloy and lime were added into liquid steel for deoxidation, alloying and slag-making during BOF tapping. (3) Liquid steel was heated in LF refining, and aluminum and lime were also added for further deoxidation and slag-making. During LF refining, the basicity of ladle slag  $w(\text{CaO})/w(\text{SiO}_2) \geq 8$ , while the mass ratio of  $w(\text{CaO})$  to  $w(\text{Al}_2\text{O}_3)$  was about 1.0–2.0. (4) After desulphurization in LF refining, FeMn alloy was added to adjust [Mn] in liquid steel, and the melt was softly blown for 6 min by argon gas with a flow rate of 600–800 L/min before LF departure. (5) Basicity of tundish flux was  $\geq 2.0$  and mass ratio of  $w(\text{CaO})$  to  $w(\text{Al}_2\text{O}_3)$  was about 1.0–1.5.

During the test, steel and slag were sampled at the stage of LF arrival, before slag-making, after slag-making, before soft blowing, LF departure and also sampled in casting tundish (about 100 tons of liquid steel was poured). The samples obtained were labelled as LF1, LF2, LF3, LF4, LF5 and CC1, respectively, as shown in Figure 1. Species were cut from the samples for the analysis of total oxygen ( $O_{\text{tot}}$ ) and inclusion inspection.

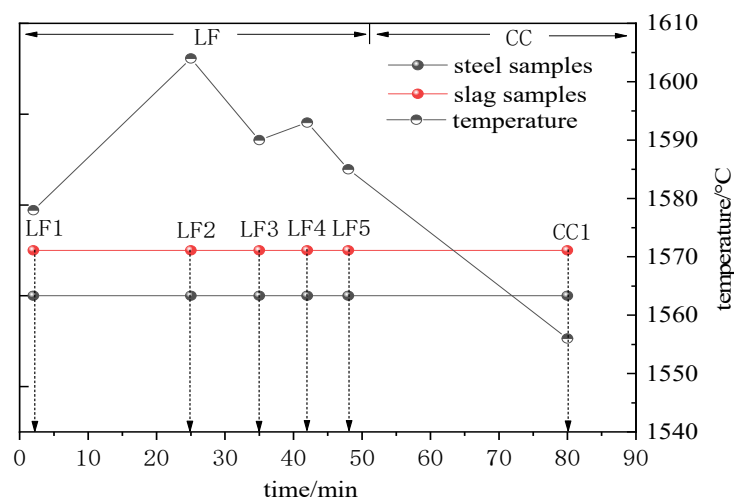


Figure 1. Schematics of samplings in the refining and casting process.

### 2.2. Laboratory Study

In order to clarify the effects of refining slag and refractory on inclusions, laboratory experiments were carried out. During the experiment, 500 g steel was put into the crucible

in a vacuum induction furnace. After vacuum extraction, purified argon gas was pumped into the furnace. The furnace was then heated to 1600 °C and steel was melted. Aluminum and 50 g slag were added into the molten steel. When the melt has been held for about 25 min, the liquid steel was tapped into a prepared ingot set in the vacuum chamber of the furnace. In order to clarify the influence of refractory on inclusions, two types of crucibles, viz. MgO ( $w(\text{MgO}) > 97.5\%$ ) and corundum ( $w(\text{Al}_2\text{O}_3) > 99\%$ ), were used in the experiments.

### 2.3. Analysis Method

Contents of  $\text{O}_{\text{tot}}$  and N in steel samples were analyzed. Inclusions  $\geq 1\mu\text{m}$  were inspected by the automatic SEM-EDS machine of ASPEX explorer, and the scanning area was about 25 mm<sup>2</sup> for each sample. According to the EDS results, Ca, Si, Al, Mn, Mg, S and O inclusions were converted into the mass percentage of the corresponding oxides and sulfides. In this paper, the attention was mainly on oxide inclusions.

## 3. Results

### 3.1. Composition of Industrial Samples

Chemical compositions of slag samples were shown in Table 1. As shown in Table 1, mass ratios of CaO/SiO<sub>2</sub> (C/S: usually named basicity) in refining slag were in the range of 13.21–29.65, and mass ratios of CaO/Al<sub>2</sub>O<sub>3</sub> (C/A) in slag were between 1.09 and 1.92. The basicity of the tundish flux was about 2.83, and the ratio of C/A was about 1.24.

**Table 1.** Chemical compositions of refining slag (wt%).

Process	Content (wt%)								C/S	C/A
	SiO <sub>2</sub>	CaO	MgO	Al <sub>2</sub> O <sub>3</sub>	MnO	P <sub>2</sub> O <sub>5</sub>	TFe	S		
LF1	3.10	45.64	4.89	38.03	1.24	0.06	3.61	0.27	14.72	1.09
LF2	3.80	55.18	4.65	29.01	0.74	0.24	1.83	0.46	13.21	1.86
LF3	2.11	57.01	4.91	30.99	0.33	0.19	1.06	0.90	27.02	1.84
LF4	1.84	57.67	4.80	30.45	0.26	0.16	0.96	0.82	31.34	1.89
LF5	1.96	58.12	4.86	30.20	0.24	0.15	1.11	0.84	29.65	1.92
CC1	13.6	38.51	9.52	31.17	1.09	0.22	1.47	0.14	2.83	1.24

Compositions of liquid steel at different stages were shown in Table 2. As can be seen, contents of Mg and Ca in steel increased with the rise of refining time, indicating a similar tendency reported by Deng et al. [21]. Mg contents were in the range of 4–7 ppm. Ca contents in steel were in the range of 3–7 ppm during LF refining, which was attributed to the reduction of CaO in slag by slag-steel chemical reactions in the refining.

**Table 2.** Compositions of steel samples (wt%).

Process	C	Si	Mn	P	S	Ca	Mg	Al <sub>t</sub>	Al <sub>s</sub>
LF1	0.040	0.016	0.165	0.014	0.014	-	0.0004	0.042	0.038
LF2	0.037	0.022	0.165	0.014	0.010	-	0.0005	0.044	0.043
LF3	0.054	0.026	0.280	0.013	0.007	0.0003	0.0004	0.055	0.053
LF4	0.054	0.026	0.286	0.014	0.006	0.0005	0.0006	0.054	0.051
LF5	0.055	0.027	0.285	0.014	0.005	0.0007	0.0007	0.052	0.048
CC1	0.056	0.025	0.278	0.014	0.005	0.0006	0.0007	0.046	0.043

### 3.2. Changes of $\text{O}_{\text{tot}}$ and N Contents in Steel

Figure 2 shows the changes of cleanliness in liquid steel. It can be seen from Figure 2 that the  $\text{O}_{\text{tot}}$  and N contents in the steel were 0.0034% and 0.0023% at LF arrival, respectively. With the proceeding of refining,  $\text{O}_{\text{tot}}$  decreased continuously while N contents increased. The lowest  $\text{O}_{\text{tot}}$  content was 0.00163%, and the N content was 0.0029% before soft blowing. At LF departure,  $\text{O}_{\text{tot}}$  and N in liquid steel were 0.0020% and 0.0033%, respectively, with an

increase of 0.0004% and 0.00042%, respectively. Compared with that before soft blowing, the pick-ups of  $O_{\text{tot}}$  and N indicated the occurrence of re-oxidation of molten steel during soft blowing. In tundish,  $O_{\text{tot}}$  and N were 0.0021% and 0.0033%, respectively. Afterwards, contents of  $O_{\text{tot}}$  and N increased by 0.00015% and 0.00005%, respectively. Despite that,  $O_{\text{tot}}$  contents in steel were controlled in the range of 0.0016–0.0022% in continuous casting.

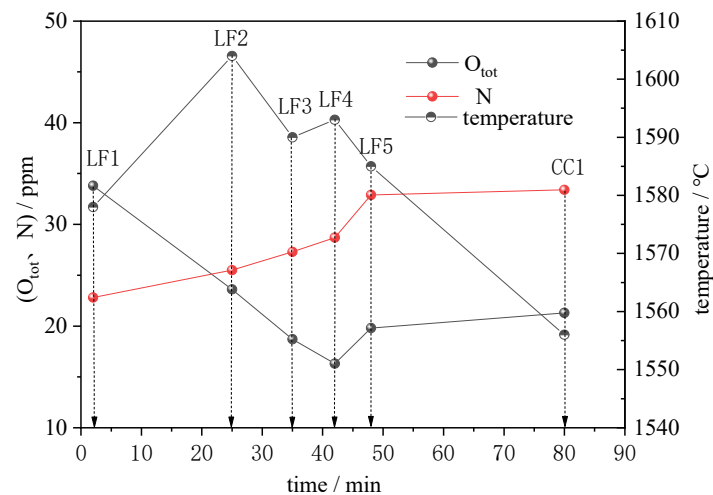


**Figure 2.** The changes of  $O_{\text{tot}}$  and N in molten steel.

### 3.3. Changes of Inclusions

#### 3.3.1. Types of Inclusions

Observed oxide inclusions can be categorized into four types:  $Al_2O_3$  (with  $Al_2O_3 \geq 95\%$ ),  $MgO-Al_2O_3$  (with  $CaO < 5\%$ ),  $CaO-MgO-Al_2O_3$  (with  $CaO \geq 5\%$ ,  $MgO \geq 5\%$ ) and  $CaO-Al_2O_3$  (with  $MgO < 5\%$ ). The number fractions of various inclusions at different times are shown in Figures 3 and 4. As can be seen, 92% of the inclusions were  $Al_2O_3$  at LF arrival, which were either in blocky or cluster shapes. Afterwards, the proportion of  $Al_2O_3$  decreased significantly to about 53%, and the fraction of  $MgO-Al_2O_3$  inclusions increased rapidly to 34%, which were mainly in irregular spheres. While the fractions of  $CaO-MgO-Al_2O_3$  and  $CaO-Al_2O_3$  were below 8%, both of which were mostly in spherical shapes, as shown in Figure 4c,d. After soft blowing, proportions of  $Al_2O_3$  and  $MgO-Al_2O_3$  inclusions decreased from 33% and 49% to 29% and 40%, respectively, while the proportions of  $CaO-MgO-Al_2O_3$  and  $CaO-Al_2O_3$  inclusions increased from 8% and 10% to 14% and 17%, respectively. In casting tundish, the fraction of  $MgO-Al_2O_3$  increased to 43%, while the fraction of  $CaO-MgO-Al_2O_3$ ,  $CaO-Al_2O_3$  and  $Al_2O_3$  increased to 15%, 20% and 22%, respectively.

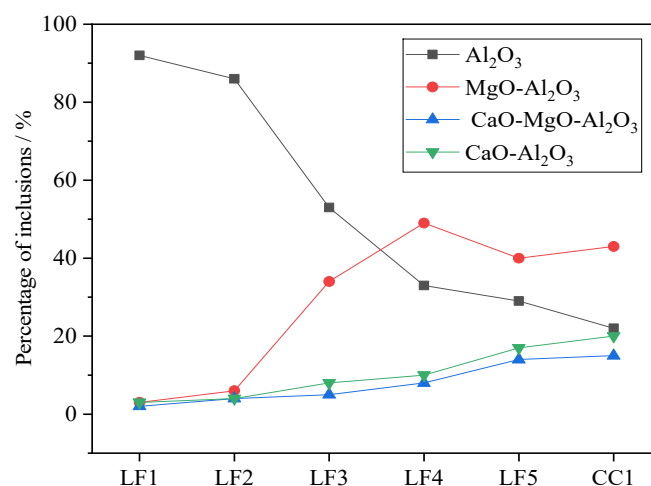


**Figure 3.** Fraction of each type of inclusions at different stages.

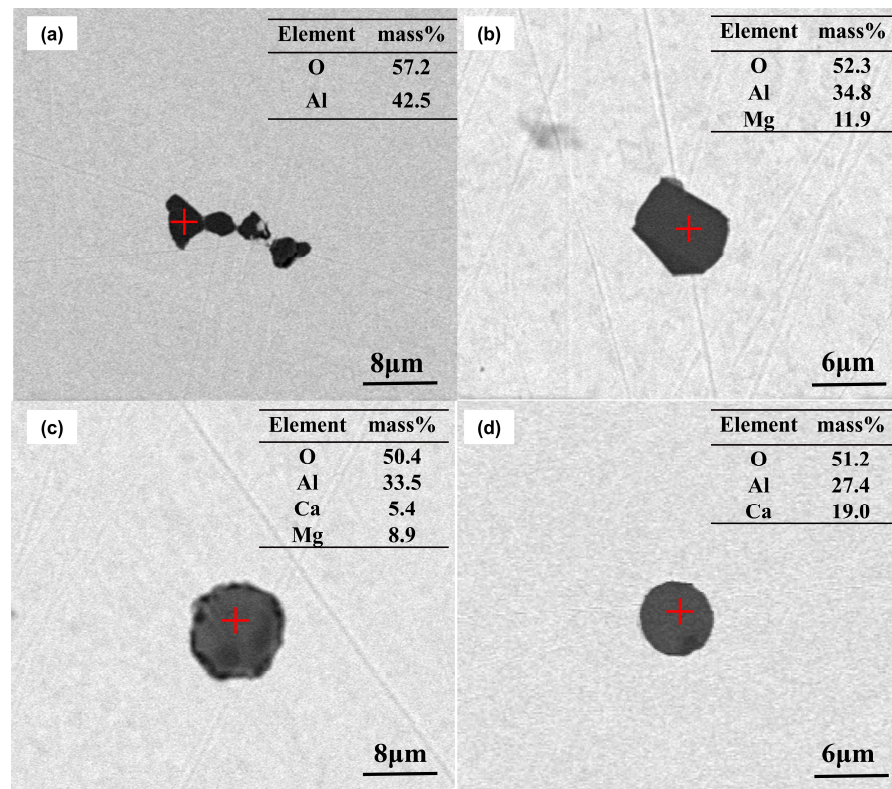


**Figure 4.** Morphology of inclusions. (a)  $\text{Al}_2\text{O}_3$ ; (b)  $\text{MgO-Al}_2\text{O}_3$ ; and (c)  $\text{CaO-MgO-Al}_2\text{O}_3$ ; (d)  $\text{CaO-Al}_2\text{O}_3$ .

### 3.3.2. Compositions of Inclusions

Compositions of inclusions at different stages were projected into  $\text{Al}_2\text{O}_3$ - $\text{MgO}$ - $\text{CaO}$  ternary phase diagram to show the evolution route of inclusions in Figure 5. Figure 5a,b suggested that inclusions at LF1 and LF2 were mainly  $\text{Al}_2\text{O}_3$ . The amounts of  $\text{MgO-Al}_2\text{O}_3$  inclusions increased gradually in sample LF3, indicating the evolution of  $\text{Al}_2\text{O}_3$  into  $\text{MgO-Al}_2\text{O}_3$ , as shown in Figure 5c,d. Before soft blowing, inclusions in steel were mainly  $\text{MgO-Al}_2\text{O}_3$ , as given in Figure 5d. Noticeably, larger  $\text{MgO-Al}_2\text{O}_3$  inclusions evolve to  $\text{CaO-MgO-Al}_2\text{O}_3$ , while smaller  $\text{MgO-Al}_2\text{O}_3$  inclusions were transformed to  $\text{CaO-Al}_2\text{O}_3$  at the stage of LF departure, as shown in Figure 5e. In casting tundish (Figure 5f), inclusions were mainly solid  $\text{MgO-Al}_2\text{O}_3$  and  $\text{CaO-Al}_2\text{O}_3$  inclusions, with sizes smaller than 10  $\mu\text{m}$ .

### 3.3.3. Quantity and Size of Inclusions

Figure 6 shows variations in the quantity and size of inclusions. It can be seen that at LF arrival, the number density of inclusions was about 13/ $\text{mm}^2$ , with an average size of about 2.8  $\mu\text{m}$ . Afterwards, the number density of inclusions reached a maximum of 17/ $\text{mm}^2$ , which could be related to more intensive argon gas bottom bubbling of ladle to promote desulfurization. Then, the number density of inclusions decreased sharply to 8/ $\text{mm}^2$ . However, the average size of inclusions slightly increased to 3.4  $\mu\text{m}$ . At LF departure, number density of inclusions was 11/ $\text{mm}^2$ , about 2/ $\text{mm}^2$  higher than that before soft blowing. Additionally, the average size of inclusions was 2.9  $\mu\text{m}$ , which was a little lower than that before soft blowing, indicating that soft blowing was favorable to the floatation of large inclusions. In the tundish, the number density of inclusions was about 10/ $\text{mm}^2$ , which was slightly lower than that of LF departure. While the average size of inclusions was 2.6  $\mu\text{m}$ , about 0.3  $\mu\text{m}$  smaller than that at LF departure.

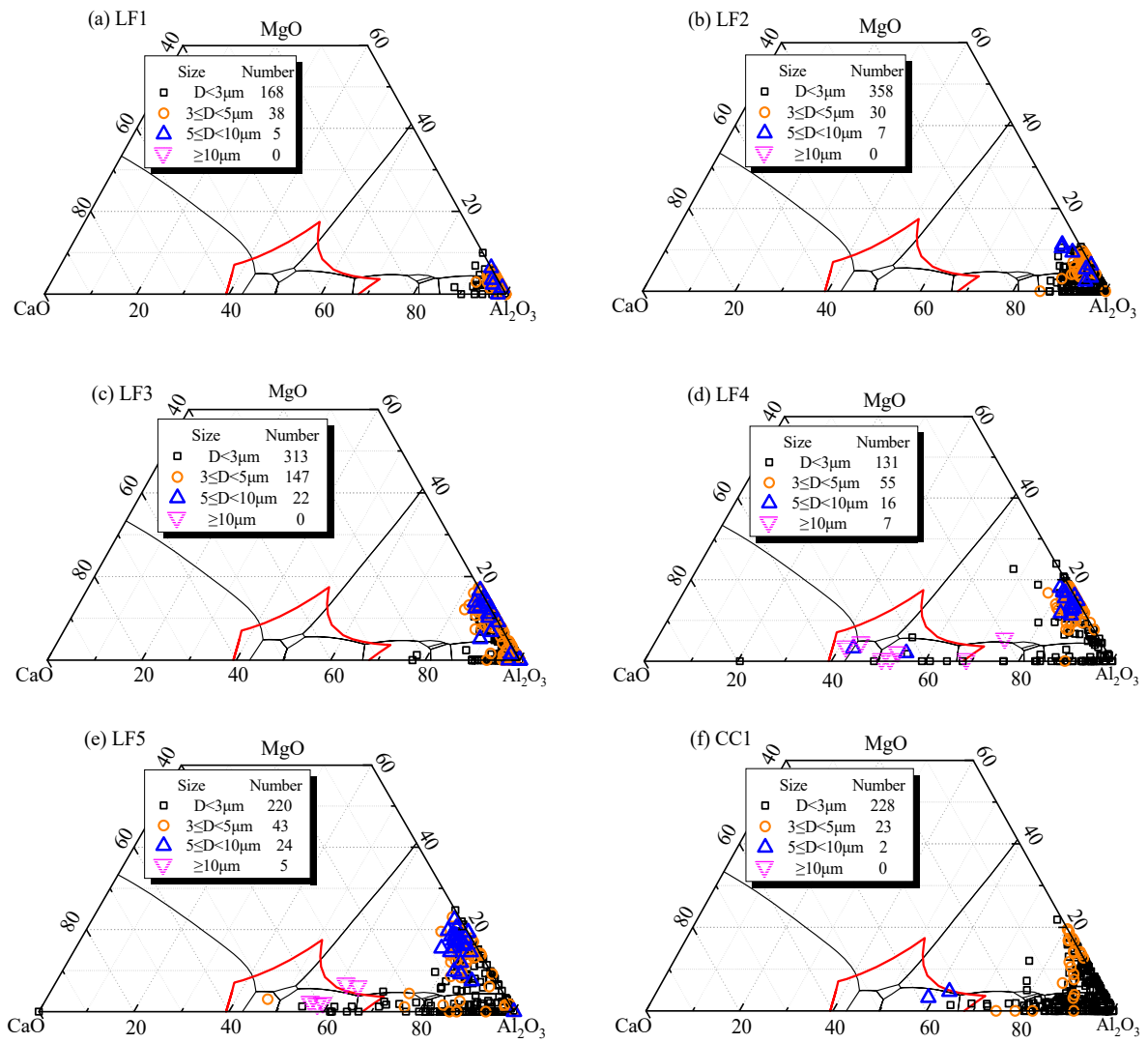


Figure 5. Evolution in the chemical compositions of inclusions in liquid steel. (a) LF1; (b) LF2; (c) LF3; (d) LF4; (e) LF5; and (f) CC1.

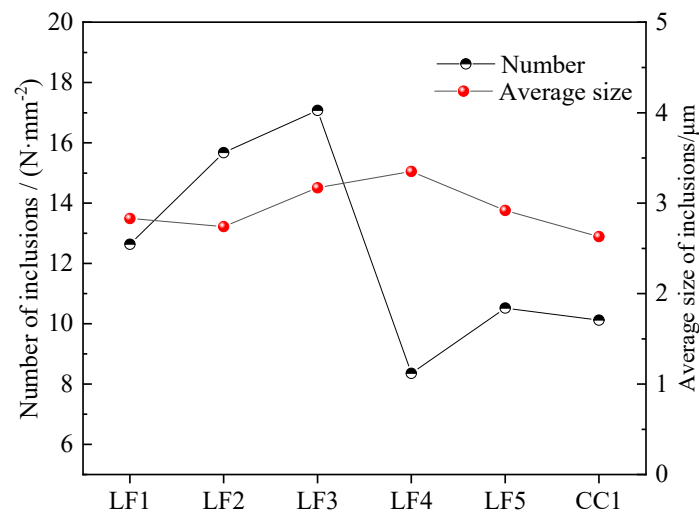
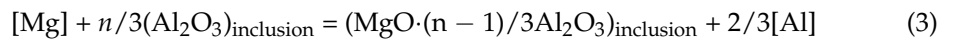
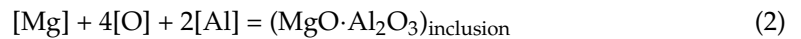
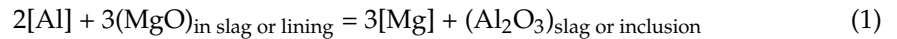


Figure 6. Number density and average size of inclusions.

## 4. Discussion

### 4.1. Formation of MgO-Al<sub>2</sub>O<sub>3</sub> Inclusions

According to previous studies, during the basic slag refining of Al-deoxidized steel, reaction (1) between [Al] in liquid steel and MgO in refining slag or ladle refractory can possibly occur [18,21–26]. Then, [Mg] reacted with [Al], [O] or Al<sub>2</sub>O<sub>3</sub> inclusions to produce MgO-Al<sub>2</sub>O<sub>3</sub>, as expressed by Equations (2) and (3) [18,27–29].



As a result, it was accepted that MgO in refining slag or ladle refractory greatly affected the formation of MgO-Al<sub>2</sub>O<sub>3</sub> inclusions [27–29].

The laboratory experiments conducted in this study clarified the influences of refining slag and choices of crucible materials (refractory) on the change of Al<sub>2</sub>O<sub>3</sub> into MgO-Al<sub>2</sub>O<sub>3</sub>. Figure 7 shows the compositions of inclusions in steel, without refining slag and with basicity of slag about 2.17 and 3.34, respectively, in which MgO crucibles were used. The inclusions were mainly MgO-Al<sub>2</sub>O<sub>3</sub> or Al<sub>2</sub>O<sub>3</sub>-MgO-CaO inclusions with a small amount of CaO. Particularly, MgO-Al<sub>2</sub>O<sub>3</sub> existed in steel even without refining slag when MgO crucible was used.

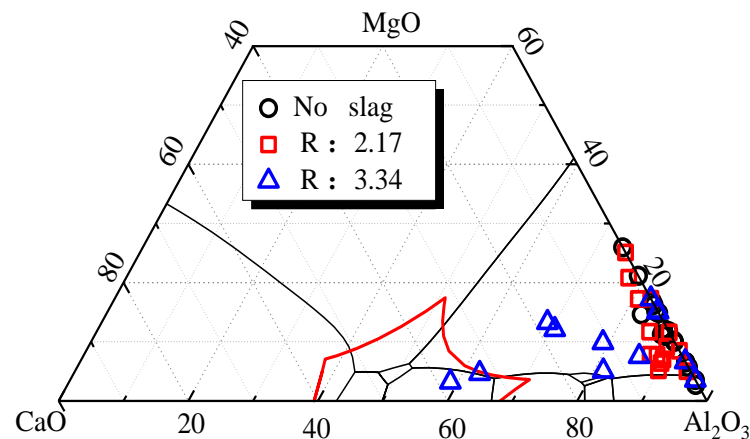


**Figure 7.** Composition of inclusions refined by different basicity slags during MgO crucible experiments.

Figure 8 shows the compositions of inclusions in steel, without refining slag and with the basicity of slag of about 4.51 and 8.24, respectively, when Al<sub>2</sub>O<sub>3</sub> crucible steel was used. As can be seen, MgO-Al<sub>2</sub>O<sub>3</sub> inclusions were well decreased, and many inclusions were composed of CaO-MgO-Al<sub>2</sub>O<sub>3</sub> with MgO contents about or within 10% when the slag contained about 5% MgO and with a basicity of about 4.5. As is known, such complex inclusions usually have lower melting points with an outer surface layer of CaO-Al<sub>2</sub>O<sub>3</sub>, which would be more desirable to enhance the castability of liquid steel. By contrast, with a slag basicity increased to 8.24, although some liquid CaO-Al<sub>2</sub>O<sub>3</sub> were formed, most inclusions were pure MgO-Al<sub>2</sub>O<sub>3</sub> inclusions or Al<sub>2</sub>O<sub>3</sub>-MgO-based ones (with CaO <5%), which were bad to the castability of molten steel.

The results clearly showed that transformation of inclusions closely related to refractory (the choice of crucible) and slag basicity. Because of larger contact area between ladle refractory and liquid steel than that between slag and liquid steel, and higher MgO activity (about 1) in the MgO-based refractory, the reaction between MgO in refractory and [Al] would be faster. It is known that MgO-Al<sub>2</sub>O<sub>3</sub> inclusions can be easily formed when MgO-crucible are used.

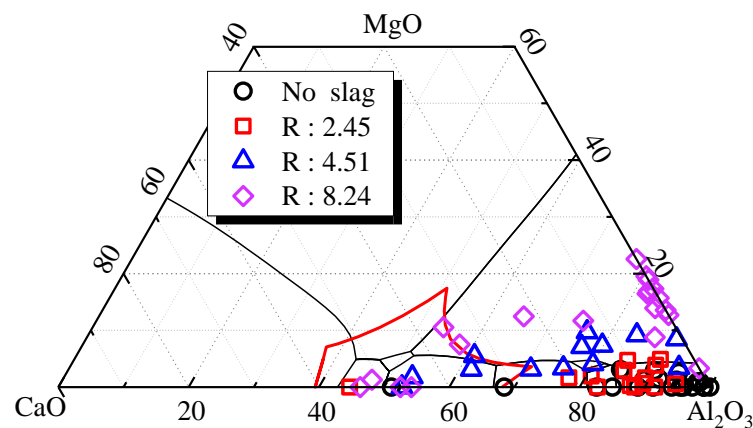
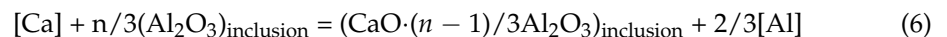
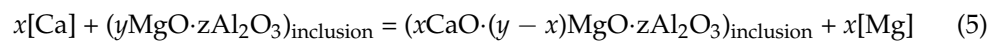
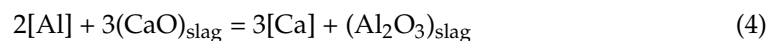


**Figure 8.** Composition of inclusions refined by different basicity slags during  $\text{Al}_2\text{O}_3$  crucible experiments.

#### 4.2. Formation Mechanism of $\text{CaO-MgO-Al}_2\text{O}_3$ or $\text{CaO-Al}_2\text{O}_3$ Inclusions

During the refining, although Ca-treatment was not used, reaction (4) could occur to supply Ca into the liquid steel [27,29–32]. Then, [Ca] would in turn react with  $\text{MgO-Al}_2\text{O}_3$  and  $\text{Al}_2\text{O}_3$  in steel to modify them into  $\text{CaO-MgO-Al}_2\text{O}_3$  or  $\text{CaO-Al}_2\text{O}_3$ , as expressed by reactions (5) and (6) [27,29,31].



With regard to the modification of  $\text{MgO-Al}_2\text{O}_3$  into  $\text{CaO-MgO-Al}_2\text{O}_3$  or  $\text{CaO-Al}_2\text{O}_3$ , previous studies showed that the transformation of  $\text{MgO-Al}_2\text{O}_3$  would proceed from the surface to the inner center, in which the rate-controlled step was the diffusion of Ca and Mg in the intermediate reaction layer [27]. In this study, variations of CaO, MgO and  $\text{Al}_2\text{O}_3$  contents in inclusions were observed, their sizes shown in Figure 9. As can be seen, higher CaO contents and lower MgO contents were observed in small inclusions. By contrast, lower CaO contents and higher MgO contents were observed in large inclusions. It implied that the modification of larger  $\text{MgO-Al}_2\text{O}_3$  inclusions needed a much longer time, which was justifiable and consistent with previous findings.

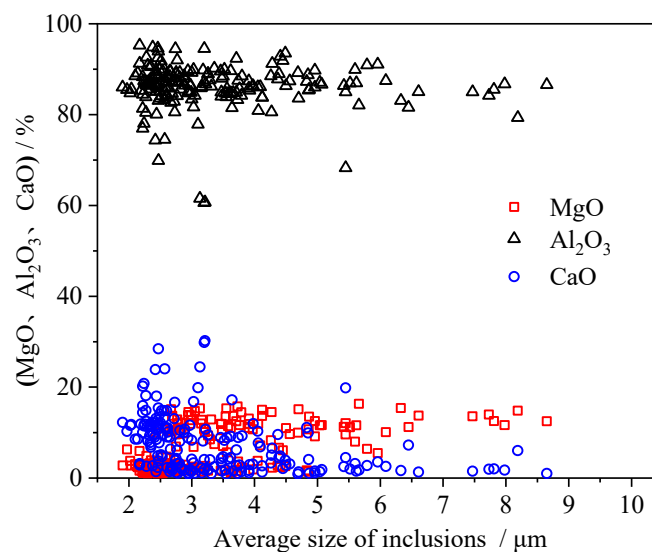


**Figure 9.** Contents of CaO, MgO and  $\text{Al}_2\text{O}_3$  in  $\text{CaO-MgO-Al}_2\text{O}_3$  inclusions.

## 5. Conclusions

This study attempted to improve the castability of LCAK by modifying solid inclusions into semi-liquid or liquid state during LF refining. It was found that evolutions of inclusions from alumina to MgO-Al<sub>2</sub>O<sub>3</sub> and then to CaO-MgO-Al<sub>2</sub>O<sub>3</sub> were hard to avoid. Evolution mechanisms of inclusions were clarified, and a possible way to reduced MgO-Al<sub>2</sub>O<sub>3</sub>-type inclusions was proposed based on laboratory experiments, in which different slags and refractories (crucibles) were used. The obtained results can be briefly concluded as follows:

1. During basic slag refining of the LCAK in with MgO lining, inclusions experienced evolutions from Al<sub>2</sub>O<sub>3</sub> → MgO-Al<sub>2</sub>O<sub>3</sub> → CaO-MgO-Al<sub>2</sub>O<sub>3</sub> → CaO-Al<sub>2</sub>O<sub>3</sub>. In the casting tundish, the number fractions of Al<sub>2</sub>O<sub>3</sub>, MgO-Al<sub>2</sub>O<sub>3</sub>, CaO-MgO-Al<sub>2</sub>O<sub>3</sub> and CaO-Al<sub>2</sub>O<sub>3</sub> inclusions were 22%, 43%, 15% and 20%, respectively. Although the transformation of solid Al<sub>2</sub>O<sub>3</sub> and MgO-Al<sub>2</sub>O<sub>3</sub> inclusions was not complete, this evolution of inclusions would be desirable to improve castability of steel, as such complex inclusions featured a lower-melting-point surface layer of CaO-Al<sub>2</sub>O<sub>3</sub> rather than solid MgO-Al<sub>2</sub>O<sub>3</sub>.
2. During the refining, CaO in the high basicity refining slag can be reduced by [Al] to supply [Ca] into steel, which afterwards helps to modify MgO-Al<sub>2</sub>O<sub>3</sub> inclusion into CaO-MgO-Al<sub>2</sub>O<sub>3</sub> or CaO-Al<sub>2</sub>O<sub>3</sub>. As the [Ca] in steel was very low and the rate-controlled step was the diffusions of Ca and Mg in spinel inclusions, smaller MgO-Al<sub>2</sub>O<sub>3</sub> largely evolved into CaO-Al<sub>2</sub>O<sub>3</sub>, while spinel inclusions in bigger sizes only changed into CaO-MgO-Al<sub>2</sub>O<sub>3</sub>.
3. The laboratory experiments revealed that when Al<sub>2</sub>O<sub>3</sub> crucibles and lower basicity refining slag (with a basicity of about 2.45) were used, MgO-Al<sub>2</sub>O<sub>3</sub> inclusions could be reduced, and the reason was understandable. During refining, [Al] would react with MgO and CaO in refining slag or MgO in refractory m to supply [Mg] and [Ca] to the steel melt. Due to the larger contact area between ladle refractory and liquid steel than that between liquid steel and slag, and because of higher MgO activity in MgO-based crucibles, the reaction of [Al] and MgO in the ladle refractory would occur much easier, which greatly contributed to the evolution of Al<sub>2</sub>O<sub>3</sub> into MgO-Al<sub>2</sub>O<sub>3</sub>. Hence, using MgO-free refractory material can effectively help decrease bad MgO-Al<sub>2</sub>O<sub>3</sub> inclusions for improved castability of liquid steel.

**Author Contributions:** Conceptualization, F.G. and X.Z.; method-ology, J.L.; software, M.J.; validation, F.W.; M.J. and J.L.; formal analysis, F.W.; investigation, F.W.; resources, F.G.; data curation, F.G.; writing—original draft preparation, F.W.; writing—review and editing, X.Z.; visualization, F.W.; supervision, X.Z.; project administration, F.W.; funding acquisition, F.G., F.W., M.J., J.L. and X.Z. All authors have read and agreed to the published version of the manuscript.

**Funding:** This research was funded by [Natural Science Foundation of China] grant number [51974017]. And The APC was funded by [51974017].

**Data Availability Statement:** Not applicable.

**Acknowledgments:** Not applicable.

**Conflicts of Interest:** The authors declare no conflict of interest.

## References

1. Zhang, L.; Lv, X.; Torgeson, A.T.; Long, M. Removal of impurity elements from molten aluminum: A review. *Miner. Process. Extr. Metall. Rev.* **2011**, *32*, 150–228. [[CrossRef](#)]
2. Li, Z.; Li, X.; Yang, L.; Shen, Z.; Wang, B.; Zhao, S.; Liang, G.; Song, C. Effect of coiling and annealing temperatures on yield point behavior of low-carbon steel. *J. Iron Steel Res. Int.* **2020**, *27*, 325–333. [[CrossRef](#)]
3. Kong, L.; Deng, Z.; Zhu, M. Reaction behaviors of Al-killed medium-manganese steel with different refractories. *Metall. Mater. Trans. B* **2018**, *49*, 1444–1452. [[CrossRef](#)]
4. Guo, J.; Cheng, S.; Cheng, Z. Characteristics of Deoxidation and Desulfurization during LF Refining Al-killed Steel by Highly Basic and Low Oxidizing Slag. *J. Iron Steel Res. Int.* **2014**, *21*, 166–173. [[CrossRef](#)]

5. Yang, W.; Zhang, L.; Wang, X.; Ren, Y.; Liu, X.; Shan, Q. Characteristics of inclusions in low carbon Al-killed steel during ladle furnace refining and calcium treatment. *ISIJ Int.* **2013**, *53*, 1401–1410. [[CrossRef](#)]
6. Lee, J.; Kang, M.; Kim, S.; Kim, J.; Kim, M.; Kang, Y. Influence of Al/Ti Ratio in Ti-ULC steel and refractory components of submerged entry nozzle on formation of clogging deposits. *ISIJ Int.* **2019**, *59*, 749–758. [[CrossRef](#)]
7. Yang, D.; Wang, X.; Yang, G.; Wei, P.; He, J. Inclusion evolution and estimation during secondary refining in calcium treated aluminum killed steels. *Steel Res. Int.* **2014**, *85*, 1517–1524. [[CrossRef](#)]
8. Alhussein, A.; Yang, W.; Zhang, L. Effect of interactions between Fe–Al alloy and MgO-based refractory on the generation of MgO·Al<sub>2</sub>O<sub>3</sub> spinel. *Ironmak. Steelmak.* **2020**, *47*, 424–431. [[CrossRef](#)]
9. Brabie, V. Mechanism of reaction between refractory materials and aluminum deoxidized molten steel. *ISIJ Int.* **1996**, *36*, 109–112. [[CrossRef](#)]
10. Zuo, X.; Long, M.; Gao, J.; Wang, Y.; Zhang, L. Inclusions and nozzle clogging during the billet continuous casting process. *Iron Steel Technol.* **2010**, *7*, 65–76.
11. Jiang, M.; Wang, X.; Chen, B.; Wang, W. Laboratory study on evolution mechanisms of non-metallic inclusions in high strength alloyed steel refined by high basicity slag. *ISIJ Int.* **2010**, *50*, 95–104. [[CrossRef](#)]
12. Yang, S.; Wang, Q.; Zhang, L.; Li, J.; Peaslee, K. Formation and modification of MgO·Al<sub>2</sub>O<sub>3</sub>-based inclusions in alloy steels. *Metall. Mater. Trans. B* **2012**, *43*, 731–750. [[CrossRef](#)]
13. Itoh, H.; Hino, M.; Ban-Ya, S. Thermodynamics on the formation of spinel nonmetallic inclusion in liquid steel. *Metall. Mater. Trans. B* **1997**, *28*, 953–956. [[CrossRef](#)]
14. Huang, F.; Zhang, L.; Zhang, Y.; Ren, Y. Kinetic modeling for the dissolution of MgO lining refractory in Al-killed steels. *Metall. Mater. Trans. B* **2017**, *48*, 2195–2206. [[CrossRef](#)]
15. Liu, Z.; Song, G.; Deng, Z.; Zhu, M. Effect of slag adjustment on inclusions in Si–Mn-killed steel during ladle furnace (LF) refining process. *Ironmak. Steelmak.* **2021**, *48*, 893–900. [[CrossRef](#)]
16. Tabatabaei, Y.; Coley, K.; Irons, G.; Sun, S. A kinetic model for modification of MgAl<sub>2</sub>O<sub>4</sub> spinel inclusions during calcium treatment in the ladle furnace. *Metall. Mater. Trans. B* **2018**, *49*, 2744–2756. [[CrossRef](#)]
17. Holappa, L.; Hämmäläinen, M.; Liukkonen, M.; Lind, M. Thermodynamic examination of inclusion modification and precipitation from calcium treatment to solidified steel. *Ironmak. Steelmak.* **2003**, *30*, 111–115. [[CrossRef](#)]
18. Pretorius, E.; Oltmann, H.; Cash, T. The Effective Modification of Spinel Inclusions by Ca Treatment in LCAK Steel. *Iron Steel Technol.* **2010**, *7*, 31–44.
19. Yang, G.; Wang, X.; Huang, F.; Wang, W.; Yin, Y.; Tang, C. Influence of Reoxidation in Tundish on Inclusion for Ca-Treated Al-Killed Steel. *Steel. Res. Int.* **2014**, *85*, 784–792. [[CrossRef](#)]
20. Peng, K.; Liu, Y.; Zhang, L. Effect of continuous oxidation on inclusions in calcium steel treatment. *China Metall.* **2018**, *28*, 16–21.
21. Deng, Z.; Liu, Z.; Zhu, M.; Huo, L. Formation, evolution and removal of MgO·Al<sub>2</sub>O<sub>3</sub> spinel inclusions in steel. *ISIJ Int.* **2021**, *61*, 1–15. [[CrossRef](#)]
22. Zhang, L.; Guo, C.; Yang, W.; Ren, Y.; Ling, H. Deformability of oxide inclusions in tire cord steels. *Metall. Mater. Trans. B* **2018**, *49*, 803–811. [[CrossRef](#)]
23. Xu, J.; Huang, F.; Wang, X. Formation Mechanism of CaS-Al<sub>2</sub>O<sub>3</sub> Inclusions in Low Sulfur Al-Killed Steel After Calcium Treatment. *Metall. Mater. Trans. B* **2016**, *47*, 1217–1227. [[CrossRef](#)]
24. Shi, C.; Yu, W.; Wang, H.; Li, J.; Jiang, M. Simultaneous modification of alumina and MgO·Al<sub>2</sub>O<sub>3</sub> inclusions by calcium treatment during electroslag remelting of stainless tool steel. *Metall. Mater. Trans. B* **2017**, *48*, 146–161. [[CrossRef](#)]
25. Park, J.; Todoroki, H. Control of MgO·Al<sub>2</sub>O<sub>3</sub> spinel inclusions in stainless steels. *ISIJ Int.* **2010**, *50*, 1333–1346. [[CrossRef](#)]
26. Ren, Y.; Zhang, L.; Zhang, Y. Modeling reoxidation behavior of Al–Ti-containing steels by CaO–Al<sub>2</sub>O<sub>3</sub>–MgO–SiO<sub>2</sub> slag. *J. Iron Steel Res. Int.* **2018**, *25*, 146–156. [[CrossRef](#)]
27. Liu, C.; Yagi, M.; Gao, X.; Kim, S.; Huang, F.; Kitamura, Y.; Ueda, S. Dissolution behavior of Mg from magnesia-chromite refractory into Al-killed molten steel. *Metall. Mater. Trans. B* **2018**, *49*, 2298–2307. [[CrossRef](#)]
28. Liu, C.; Gao, X.; Kim, S.; Ueda, S.; Kitamura, S. Dissolution behavior of Mg from MgO–C refractory in Al-killed molten steel. *ISIJ Int.* **2018**, *58*, 488–495. [[CrossRef](#)]
29. Harada, A.; Miyano, G.; Maruoka, N.; Shibata, H.; Kitamura, S. Dissolution behavior of Mg from MgO into molten steel deoxidized by Al. *ISIJ Int.* **2014**, *54*, 2230–2238. [[CrossRef](#)]
30. Wang, X.; Li, X.; Qiang, L.; Huang, F.; Jian, Y. Control of Stringer Shaped Non-Metallic Inclusions of CaO–Al<sub>2</sub>O<sub>3</sub> System in API X80 Linepipe Steel Plates. *Steel. Res. Int.* **2014**, *85*, 155–163. [[CrossRef](#)]
31. Liu, C.; Gao, X.; Ueda, S.; Guo, M.; Kitamura, S. Composition changes of inclusions by reaction with slag and refractory: A review. *ISIJ Int.* **2020**, *60*, 1835–1848. [[CrossRef](#)]
32. Yu, H.; Qiu, G.; Zhang, J.; Wang, X. Effect of Medium Basicity Refining Slag on the Cleanliness of Al-killed Steel. *ISIJ Int.* **2021**, *61*, 2882–2888. [[CrossRef](#)]

**Disclaimer/Publisher’s Note:** The statements, opinions and data contained in all publications are solely those of the individual author(s) and contributor(s) and not of MDPI and/or the editor(s). MDPI and/or the editor(s) disclaim responsibility for any injury to people or property resulting from any ideas, methods, instructions or products referred to in the content.